# Comparison of Dynamic Lattice Monte Carlo Simulations and the Dielectric Self-Energy Poisson−Nernst−Planck Continuum Theory for Model Ion Channels

**Peter Graf,[†] Maria G. Kurnikova,[‡] Rob D. Coalson,*[,§] and Abraham Nitzan[†]**

*Chemistry Department, University of Tel Aviv, Tel Aviv, Israel, Chemistry Department, Carnegie Mellon University, Pittsburgh, Pennsylvania 15213, and Chemistry Department, University of Pittsburgh, Pittsburgh, Pennsylvania 15260*

*Received: June 2, 2003; In Final Form: October 7, 2003*

Simulations of ion permeation through narrow model cylindrical channels are carried out using a dynamic lattice Monte Carlo (DLMC) algorithm (equivalent to high friction Langevin dynamics) for the time evolution of the ions in the system on the basis of a careful evaluation of the electrostatic forces acting upon each particle. To mimic the process of ion transport through protein channels, the cylindrical channel is embedded in a dielectric slab (representing a lipid bilayer membrane). The protein/membrane structure is taken to be rigid, and the water solvent is treated as a dielectric continuum. Results of these simulations are compared to corresponding results obtained via Poisson−Nernst−Planck (PNP) theory. In the PNP approach, the mobile ions are treated as a continuous charge density, and the electrostatic force on each ion is treated in an approximate fashion. Significant differences between DLMC and PNP results are found, with the degree of discrepancy increasing as the radius of the ion channel is reduced. A major source of error is traced to the neglect in the effective PNP potential of the dielectric self-energy (DSE), which is due to the interaction of each permeant ion with the dielectrically inhomogeneous environment provided by the water/channel/membrane system. When this static single-particle potential is precalculated and added to the effective potential used in PNP theory, substantial improvement in the quality of the results for current−voltage curves and steady-state concentrations is obtained. In fact, the results obtained by this approach, termed dielectric self-energy Poisson−Nernst−Planck (DSEPNP) theory, agree nearly quantitatively with DLMC simulation results over the entire range of channel radii (4−12 Å) studied.

## 1. Introduction

Recently, several groups have carried out Brownian dynamics (BD) or dynamic lattice Monte Carlo (DLMC) simulations to calculate currents through biological channels via a physically realistic model in which permeant ions are represented as hard spheres with an embedded electric charge.[1−11] One important goal of these studies has been to elucidate the behavior of ion kinetics through narrow ion channels (several angstroms in radius), which have significant biological relevance (e.g., as selectivity filters). In such narrow ion channels, these calculations predict very small superlinear currents for voltages up to 200 mV. Curiously, the computed $I-V$ curves[4,12] do not closely resemble those measured experimentally,[13,14] which are typically linear or sublinear rather than superlinear in shape and much larger in magnitude. Also curious is the fact that in many cases a cruder model of ion permeation known as Poisson−Nernst−Planck (PNP) theory, in which the ions are treated as a continuous charge density and ion−ion interactions are treated within a mean-field approximation, predicts qualitatively reasonable ion currents through narrow biological ion channels.[15−20]

Particle-based Brownian dynamics models are clearly more realistic than the continuum/mean-field PNP theory in several respects. In BD models, the ions have a finite size and thus are forced to traverse a narrow channel (e.g., gramicidin[21] or the KcsA channel[22]) in essentially single-file fashion. Furthermore, all ion−ion interactions are computed accurately (within the model of a rigid protein, dielectric continuum representation of the solvent, etc.) at each instant of time. Thus, the many-body nature of the ionic motion is properly described. Basic PNP theory, on the other hand, describes mobile ionic charge by a continuous distribution, effectively regarding the individual carriers as infinitesimal in charge (as well as in size) and infinite in number, taking only the charge density as given. Furthermore, it is implicitly assumed in PNP theory that the steady-state ion concentration profile is characterized by negligible spatio-temporal fluctuations so that each ion "sees" a static charge distribution due to the other ions−that is, a mean-field approximation is adopted in order to treat mobile ion−ion interactions.

Despite the additional realism in Brownian dynamics-type calculations, they are at present still far from being ab initio. There are several significant approximations inherent in this approach as it is most often implemented at present. First, the protein (and lipid bilayer) are considered to be static objects, whereas they are in fact dynamical. They undergo fluctuations on a picosecond time scale, which is much more rapid than the time scale for ion permeation (several nanoseconds or longer). Thus, protein atoms can relax instantaneously around the ion as it moves through the channel, and this conformational "polarization" can stabilize the permeant ion by minimizing strong short-range electrostatic interactions between the ion and nearby protein atoms. Furthermore, the solvent (i.e., water) is treated as a dielectric continuum in BD simulations. Because a water molecule is approximately the same size as a $K^+$ or $Cl^-$ ion, the separation of time/distance scales implicit in a model of Brownian motion (in which the ion is the "Brownian particle"

* Corresponding author. E-mail: coalson@pitt.edu.
[†] University of Tel Aviv.
[‡] Carnegie Mellon University.
[§] University of Pittsburgh.

10.1021/jp0355307 CCC: $27.50 
Published on Web 01/17/2004

and the water is the "source of thermal buffeting") is not fully justified. These issues are exacerbated when a few water molecules and a few ions are confined to a narrow ion channel. Of course, the same assumptions, namely, treating the protein as a static object and the water solvent as a dielectric continuum, plague the continuum PNP theory as well.

Recent work[23] suggests that two competing effects, both left out of standard PNP theory, compensate each other and in some cases approximately cancel out, thus explaining why standard PNP calculations are often "unjustifiably" successful in reproducing experimental data. One effect is the dielectric self-energy (i.e., the electrostatic energy of a single mobile ion moving in a dielectrically inhomogeneous environment[24]). In particular, when an ion enters the aqueous pore of the protein channel, it is surrounded "on the sides" by the low-dielectric environment of the surrounding protein/membrane. Thus, the electrostatic energy increases as the ion goes further into the channel (maximizing when the ion is "most buried", i.e., halfway through the pore). The magnitude of this dielectric barrier can be quite significant—the narrower the ion channel, the greater the effect. For gramicidin (radius of ca. 2Å), the dielectric barrier for a monovalent ion is $\sim 20\ kT$.[23] In the absence of some compensating stabilizing mechanism, no ions would flow through this channel, which contradicts the experimental reality that gramicidin passes millions of cations per second under physiologically relevant conditions. The effect of dielectric self-energy on ion permeation has been recognized and extensively discussed in earlier ion-channel literature, even though the three-dimensional structure of actual protein pores was in general not known at the time.[25−33] One potentially compensating mechanism is the relaxation of the protein channel itself around the ion as it passes through the pore. As noted above, this protein stabilization, which involves small (sub-angstrom) shifts in the position of nearby protein atoms, can occur on a picosecond time scale and via slight movement of partial charges on the protein provide significant electrostatic stabilization. Physically, this distortion of the protein atoms closely resembles the mechanism by which the atomic lattice of a crystal distorts to stabilize a free electron moving through it (i.e., polaron formation[34]).

The above scenario is complex, and it is thus important to decompose it into component contributions and analyze each of these carefully. In this paper, we adopt the "standard" model of ion permeation through a protein channel, namely, one in which the protein itself (as well as the lipid bilayer membrane in which it sits) is represented as a rigid dielectric slab characterized by a low dielectric constant and pocked with point charges embedded at various locations to represent (partial) charges in the protein/membrane. Furthermore, the water solvent is treated as a permeable dielectric medium characterized by a dielectric constant and an appropriate viscosity. Within this model, we carry out accurate DLMC simulations based on the instantaneous force on each ion, taking into account all electrostatic interactions. The results of these calculations serve as a benchmark against which to test standard PNP theory and variants on the PNP theme. Indeed, we find that standard PNP calculations deviate significantly from the DLMC results—the disagreement becomes worse as the radius of the ion channel becomes narrower. We trace the disagreement to the neglect of the DSE in standard PNP theory. Furthermore, we find that by "putting in" the DSE energy function as an additional single-particle potential in the PNP equations (an approximation that will be termed DSEPNP) the agreement with DLMC simulations improves dramatically, becoming nearly quantitative over the entire range of ion channel radii studied (from 4 to 12 Å).

The outline of the paper is as follows. To set the stage, we briefly review the structure of standard PNP theory in section 2, and in Section 3, we describe a simple procedure for incorporating the DSE into PNP (i.e., DSEPNP). Our reasoning here closely follows that of Schuss et al.[35] Our DLMC algorithm is outlined in section 4. In section 5, we compare the results of PNP and DSEPNP with our DLMC simulation data. The paper concludes, in section 6, with a discussion of our findings.

## 2. Continuum Models: PNP Theory

At the simplest level of the theory of drift diffusion in an inhomogeneous environment such as an ion channel, the mobile ions are treated as a continuous distribution. The concentrations of these ions are therefore described by a set of partial differential equations, termed drift-diffusion or Nernst−Planck (NP) equations, one for each ionic species. In particular, the local flux $\vec{j}_I$ is given by

$$-\vec{j}_I(\vec{r}) = D_I(\vec{r})\left[\frac{\partial c_I(\vec{r})}{\partial \vec{r}} + \beta c_I(\vec{r})\frac{\partial \psi_I(\vec{r})}{\partial \vec{r}}\right] \qquad (1)$$

where $c_I$ is the concentration of species $I$ and $q_I$ is the charge on an ion of this type. Furthermore, $\psi_I$ is an appropriate effective potential energy experienced by each particle of species $I$, $D_I$ is the diffusion constant (possibly position-dependent) for this species, and $\beta = (kT)^{-1}$, $k$ being Boltzmann's constant and $T$ the absolute temperature. The time evolution is then given in general by the continuity equation[36] $\partial c_I/\partial t = -div(\vec{j}_I)$. Here we are primarily interested in the steady-state profile satisfying $div(\vec{j}_I) = 0$, which constitutes the NP equation for species $I$.

The details of $\psi$ obviously play a critical role in this description. Most properly, $\psi_I(\vec{r})$ should be thought of as a potential of mean force[36] for a single mobile ion of species $I$ because this generates a Boltzmann distribution [proportional to $\exp(-\beta\psi_I(\vec{r}))$] in the case of a zero-flux steady state corresponding to thermal equilibrium. Of course, $\psi_I(\vec{r})$ depends on a complicated average over all mobile ions in the system. Thus, it is natural to seek simplified approximations to this free-energy function. The simplest plausible approximation follows upon considering contributions to the force on a typical mobile particle including the electric fields produced by all other charges in the system, plus impenetrable hard walls of the pore/membrane structure. We may distinguish three types of free charges in the system: mobile ions, immobile (partial) charges embedded in the protein/membrane, and charges on the distant capacitor plates of the probing electrodes. The electric field of the fixed ions is easily calculated (including effects of dielectric inhomogeneity). The electric field from the charges in the external capacitor plates can be subsumed into a solution of the Laplace equation with boundary conditions that enforce fixed electric potential values on the capacitor plates. This leaves the mobile charges. The force on a test ion due to the other mobile ions in the system depends on the instantaneous configuration of all mobile particles. As a crude approximation, we can assume that the number density of mobile ions at each point in space is frozen at its steady state (average) value (further subtleties in this reasoning are discussed below) and calculate the electric field at position $\vec{r}$ due to the corresponding steady-state charge distribution. The sum of all of the electrostatic forces can be obtained from the gradient of the electric potential field that satisfies the following Poisson equation:

$$\vec{\nabla}\cdot(\varepsilon(\vec{r})\vec{\nabla}\phi(\vec{r})) = -4\pi\left(\rho_f(\vec{r}) + \sum_I q_I c_I(\vec{r})\right) \qquad (2)$$

where $\rho_f(\vec{r})$ is the density of immobile charges in the system (i.e., partial charges on the lipid bilayer membrane and the protein molecule). The appropriate boundary condition on the surface of the "computational box" is a fixed surface potential that incorporates the potential difference across the membrane supplied by the electrodes. Then, for each species of mobile ion there is one Nernst−Planck equation (eq 1 above with $\psi_I \rightarrow q_I\phi$). The boundary conditions on each NP equation enforce the bulk concentrations in the bathing solutions on either side of the membrane. For internal boundary surfaces (e.g., the surface of the membrane and the inner walls of the protein), zero-flux boundary conditions are utilized. This set of NP equations (cf. eq 1), one for each ionic species, plus one Poisson equation (eq 2) constitutes a nonlinear set of partial differential equation that are the embodiment of standard PNP theory.[15−20,37]

### 3. Dielectric Self-Energy Poisson−Nernst−Planck (DSEPNP) Theory

When an ion moves through a dielectrically inhomogeneous medium, it experiences a force due to the variation of the dielectric self-energy (DSE) with the position of the ion. In particular, the DSE of an ion increases as it moves from the bulk solvent, where it is surrounded by a high-dielectric medium (water), to the inside of a narrow ion channel, where it is surrounded by a low-dielectric medium (the protein/membrane system). Note that this force persists even in the absence of any other free charges in the system. If there are $N$ charges in total and we are interested in the net force on the $n$th charge without (for the moment) any applied external electric potential, then the analysis performed in Appendix 1 shows that this force is the negative of the gradient of the following energy function:

$$\mathcal{E}(\vec{R}_n) = q_n \sum_{j\neq n} q_j g(\vec{R}_n,\vec{R}_j) + \frac{1}{2} q_n^2 g(\vec{R}_n,\vec{R}_n) \tag{3}$$

In this expression, $g(\vec{R}_n,\vec{R}_j)$ is the potential generated at point $\vec{R}_n$ by a unit source charge at $\vec{R}_j$, subject to the boundary condition that $g \rightarrow 0$ far from $\vec{R}_j$. Thus, the first term accounts for the electric field at point $\vec{R}_n$ generated by the other $N-1$ point charges (mobile and immobile charges enter on the same footing here). The second term is the DSE, which varies with position in a dielectrically inhomogeneous medium, thus giving rise to a nonzero force on ion $n$.

As noted above, the electric field contributed by external electrodes can be obtained by solving the Laplace equation with appropriate "fixed potential" boundary conditions and then differentiating the resultant electric potential field. Hence, the force on particle $n$ due to all other free charges in the system plus the applied electric field from external capacitors (electrodes) can be obtained by differentiating the scalar potential field $\varphi_0$ computed from a *single* Poisson equation, namely,

$$\vec{\nabla}\cdot(\varepsilon(\vec{r})\vec{\nabla}\varphi_0(\vec{r})) = -4\pi \sum_{j\neq n} q_j \delta(\vec{r} - \vec{R}_j)$$

subject to the boundary condition that $\phi_0(\vec{r}) = \phi_{bc}(\vec{r})$ on the system boundaries.

To this must be added the force due to the spatial variation of the DSE. The net force on particle $n$ (including the electric field from the external electrodes, the fields generated by all other free charges in the system, and the DSE) is thus given as the negative of the gradient of the following potential energy function:

$$\psi = q_n\phi_0(\vec{R}_n) + \mathcal{E}_{DSE}(\vec{R}_n) \tag{4}$$

with

$$\mathcal{E}_{DSE}(\vec{R}_n) = \frac{1}{2} q_n^2 g(\vec{R}_n,\vec{R}_n)$$

This expression is exact, but if there are mobile free charges (ions) in the system, it depends on the instantaneous configuration of all ions except the "test" ion $n$. Thus, one must reevaluate it every time a particle is moved (as in DLMC simulations) or else approximate it as a functional of an average mobile ion density (as in PNP theory). To do the latter, it is useful to specialize to the case that there are $N_m$ mobile ions and $N_f$ fixed charges (cf. Figure 1). Then

$$\sum_{j\neq n} q_j \delta(\vec{R}_n - \vec{R}_j) = \rho_f(\vec{R}_n) + \rho_m(\vec{R}_n) \tag{5}$$

where

$$\rho_f(\vec{R}_n) \equiv \sum_{k=1}^{N_f} q_k \delta(\vec{R}_n - \vec{R}_k) \tag{6a}$$

and

$$\rho_m(\vec{R}_n) \equiv \sum_{j\neq n} q_j \delta(\vec{R}_n - \vec{R}_j) \tag{6b}$$

(The summation that determines $\rho_m$ includes all $N_m$ mobile charges except the $n$th charge.) Clearly, in eq 6, $\rho_f(\vec{R}_n)$ is an externally prescribed charge distribution, and $\rho_m(\vec{R}_n)$ depends on the instantaneous configuration of all mobile ions. It is the latter term that requires further attention. The approximation sequence that is necessary to obtain a tractable mean-field theory is

$$\rho_m(\vec{R}_n) \rightarrow \left\langle \sum_{j\neq n} q_j \delta(\vec{R}_n - \vec{R}_j) \right\rangle \rightarrow \left\langle \sum_{j=1}^{N} q_j \delta(\vec{R}_n - \vec{R}_j) \right\rangle \equiv \bar{\rho}_m(\vec{R}_n) \tag{7}$$

where $\bar{\rho}_m$ is the average net charge density profile

$$\bar{\rho}_m(\vec{r}) = \sum_I q_I c_I(\vec{r}) \tag{8}$$

thus yielding a closed set of equations for the species concentrations.

Essentially, we have just sketched the "derivation" of classical PNP theory, warts and all. The new development is the identification of an additional single-particle potential, the dielectric self-energy (DSE), which does not appear in traditional PNP discussions. Because this really is a static single-particle potential, it can be added to the effective potential utilized in the NP part of the PNP equations.

For clarity, we summarize here the final modified DSEPNP prescription: The concentration profile of each ion species $I$ satisfies a Nernst−Planck equation

$$0 = \vec{\nabla}\cdot\{D_I(\vec{r})[\vec{\nabla}c_I(\vec{r}) + \beta c_I(\vec{r})\vec{\nabla}\psi_{eff,I}(\vec{r})]\} \tag{9}$$

The effective potential seen by each ion species is

$$\psi_{eff,I}(\vec{r}) = q_I\phi(\vec{r}) + \mathcal{E}_{DSE,I}(\vec{r}) \tag{10}$$

Here, $\phi$ is the solution to the Poisson equation:

$$\vec{\nabla}\cdot(\varepsilon(\vec{r})\vec{\nabla}\phi(\vec{r})) = -4\pi[\rho_f(\vec{r}) + \bar{\rho}_m(\vec{r})] \tag{11}$$

with the fixed charge density $\rho_f$ given in eq 6a, the net mobile ion charge density $\bar{\rho}_m$ given in eq 8, and the boundary condition $\phi(\vec{r}) = \phi_{bc}(\vec{r})$ on the various bounding surfaces of the simulation box. Furthermore, the dielectric self-energy function for ion species $I$ is given by

$$\mathcal{E}_{DSE,I}(\vec{r}) = \frac{1}{2}q_I^2 g(\vec{r},\vec{r}) \tag{12}$$

The NP equations for all species (cf. eq 9) and the Poisson equation (eq 11) must then be solved to self-consistency.

The above arguments are similar to the ones used in the discussion of the replacement of conditional by unconditional charge densities in ref 35. Our presentation emphasizes that the effective potential that determines the force on an ion due to the induction of surface charge in a dielectrically inhomogeneous medium is given as the negative gradient of the DSE potential defined herein (i.e., $\mathcal{E}_{DSE,I}(\vec{r}) = (1/2)q_I^2 g(\vec{r},\vec{r})$. Its inclusion is consistent with the way in which we perform our DLMC simulations (see section 4) and also with the way in which free energies of solvation are typically computed in continuum solvent models (cf. ref 38). Note that in order to make one dynamical move in our DLMC algorithm we need to evaluate the electrostatic energy of the system twice: before and after a trial move of the particle is attempted. Thus, formally we must solve the Poisson equation for the electric potential generated by an (ionic) point source two times in order to calculate the DSE contribution to the relevant energetics. [In practice, these DSE evaluations can be precalculated and stored on the computational grid (cf. section 4).] Even in the absence of any other source charges in the system, mobile or immobile, a reevaluation of the DSE in this manner is required. In essence, the difference between the DSE at initial and trial-move positions of the ion (divided by the separation between these positions) gives the instantaneous force exerted on the ion by the induced charges at the dielectric boundaries. In the formulation of Schuss et al.,[35] a different prescription for this dielectric boundary force is given. In particular, it is obtained from a single solution of the Poisson equation for a point source charge at the initial ("current") position of the ion. From the resultant electric potential profile, the dielectric boundary force is extracted (by evaluating the gradient of this potential in an appropriate manner). Although it may not be immediately obvious that the two prescriptions give the same force, in fact they do: a simple equivalence proof is provided in Appendix 2. Which prescription is employed in a given calculation is a matter of convenience and computational efficiency.

In concluding this section, note that in the limit where a continuous charge distribution is obtained by reducing the charge per mobile particle and increasing the number of mobile particles concomitantly (such that the charge density remains constant) the DSE effect becomes negligible. The DSE scales as the square of the charge on a single mobile particle, and this charge tends to zero in the limit process just described. Thus, DSEPNP theory reduces to standard PNP theory in this limit.

## 4. Dynamic Monte Carlo Simulations

The details of the DLMC procedure used here were thoroughly described in previous work.[4] In this method, the system of particles evolves in time according to the transition probability algorithm often used in dynamic Ising model simulations.[39] Given a current configuration 1 and a random trial configuration 2, the criterion for choosing the next configuration as 2 or 1 depends on the energy difference $\Delta W$ between these configurations. A uniform random deviate $0 \le r < 1$ is generated. If

$$r < \frac{1}{1 + \exp[\beta\Delta W]} \tag{13}$$

then the next configuration is taken to be 2. Otherwise, the current configuration 1 is carried over. The energy of the system was calculated as the following sum:

$$W = W^{\text{stat}} + W^{\text{self}} + W^{\text{coul}} + W^{\text{diel}} + W^{\text{corr}} \tag{14}$$

where each energy term is defined below. The details of how various energy contributions are calculated are described elsewhere.[4] The first term (the sums below are over all ions in the computational box)

$$W^{\text{stat}} = \sum_j q_j \phi_j^{\text{stat}} \tag{15}$$

is the energy of individual ions in the local electrostatic field arising from static charges and from the source of the imposed (Dirichlet) boundary condition. Next, the term

$$W^{\text{self}} = \sum_j \frac{q_j^2}{2}\phi_j^{\text{self}} \tag{16}$$

is the self-energy (or solvation energy) of individual ions in the inhomogeneous dielectric environment.

Turning to the ion−ion interaction, it is convenient to separate it into two terms. The first

$$W^{\text{coul}} = \frac{1}{2}\sum_{i\neq j}\frac{q_i q_j}{\varepsilon_B}\phi^{\text{coul}}(r_{ij}) \tag{17}$$

is due to the direct Coulombic interaction between pair of ions in a reference homogeneous dielectric environment with dielectric constant $\varepsilon_B$. A second term

$$W^{\text{diel}} = \frac{1}{2}\sum_{i\neq j} q_i q_j \phi_{i\leftarrow j}^{\text{diel}} \tag{18}$$

is the energy resulting from pair of ions interacting via polarization charges induced at internal dielectric interfaces.

$$W^{\text{corr}} = \sum_j \langle \Phi_j^{\text{corr}} \rangle \tag{19}$$

is a correction to the solvation energy that accounts for the effects of ions outside the inner (primary) system.

The simulation procedure was implemented on a lattice as described in ref 4 where each mobile ion can occupy one lattice cell. The total simulation time $T_S$ is related to the total number of Monte Carlo cycles $N_C$ as

$$T_S = \frac{h^2 N_C}{12D} \tag{20}$$

where $h$ is the grid spacing and $D$ is the diffusion coefficient of a single ion moving in the dielectric environment. The latter is taken to be the same for all mobile ions and is assumed to be

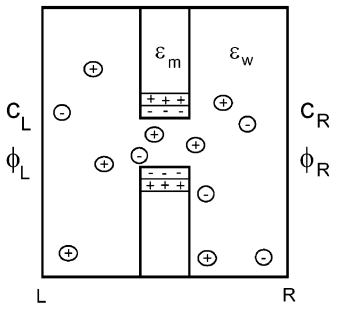


**Figure 1.** Two-dimensional cross section of the 3D DLMC simulation box depicting an assembly of free charges in a dielectrically inhomogeneous medium. Note that some free charges (encircled) are mobile and that others (in the dielectric region with $\varepsilon_m$) are fixed in space.

known. $D = 10^{-5}$ cm$^2$/s was used in all the calculations presented in this work.[44]

A cycle is defined to consist of $\tilde{N}$ steps with $\tilde{N} = N + N_v$. $N$ is the number of ions in the system, which may fluctuate with time. The total number of particles must, however, be kept constant to ensure the consistent accounting of time; therefore, the number of virtual particles $N_v > 0$ is chosen such that $\tilde{N}$ is a constant.

## 5. Comparison of DLMC Simulations versus PNP and DSEPNP Calculations on a Model 3D Ion-Channel System

We consider a 3D model ion-channel/membrane system depicted schematically in Figure 1. The protein channel is represented as a cylinder of specified radius and length. This cylinder spans a dielectric slab, which approximates a lipid bilayer, in a perpendicular fashion. The cylinder is lined with two layers of charge: an inner layer (closest to the aqueous pore) of total charge $-1.5e$, which is surrounded by a second layer of total charge $1.5e$. These charge distributions mimic the arrangement of polar groups that line cationic channels. For example, in gramicidin, carbonyl groups from the peptide backbone are oriented along the aqueous pore region, with the (electronegative) oxygen atom of each carbonyl group pointing inward. The model adopted here is not intended to represent precisely the gramicidin protein channel, but the presence of a layer of negative charge on the innermost lining of the channel contributes significantly to the mechanism by which cations are drawn into and ultimately passed through it, so it is important to include this feature in our idealized channel model.

The channel/membrane/water system under study is dielectrically inhomogeneous. Roughly, the water is a high-dielectric medium ($\varepsilon_w = 80$), and the protein/membrane complex, being composed largely of low-polarizability alkane chains and other organic moieties, is a low-dielectric medium ($\varepsilon_m = 2$). In reality, the situation is more complicated. Whereas bulk water is indeed characterized by a static dielectric constant of 80, the appropriate dielectric constant in the pore interior is not known experimentally. Given the highly confined geometry associated with narrow ion channels (less than 5 Å in radius), the invocation of a dielectric continuum description of the water in the channel is itself questionable. Ignoring this potential dilemma, the precise value for the dielectric constant of water in the interior of the channel remains an issue. Presumably, it is lower than the bulk value because the ability of the confined water to rotate is restricted and hence its rotational polarizability is reduced. Furthermore, whereas the dielectric constant of the alkane chain-dominated lipid layer is probably well represented by a dielectric

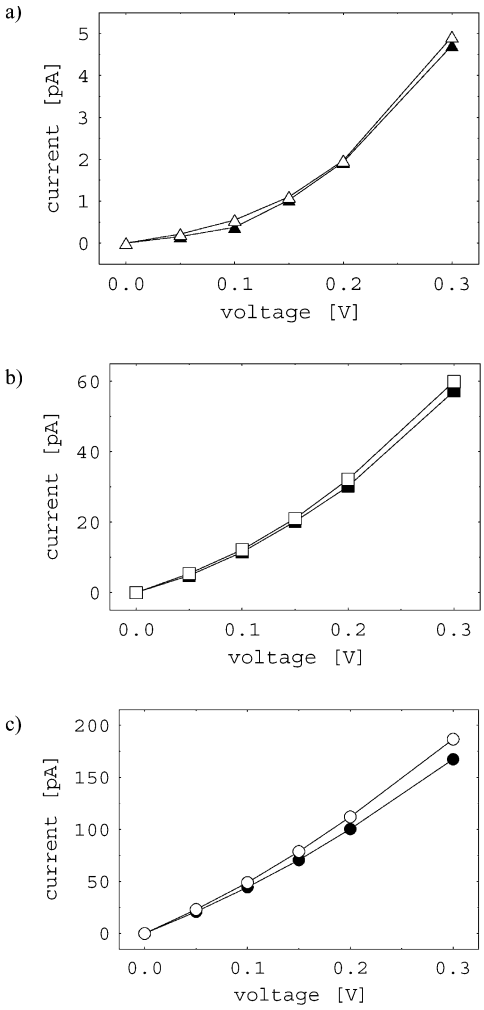


**Figure 2.** Comparison of current−voltage characteristics calculated for the ion channel shown in Figure 1 via DLMC (filled symbols) and DSEPNP (open symbols) methods for channel radii of (a) 0.4 nm, (b) 0.75 nm, and (c) = 1.2 nm. The choice of dielectric constants, fixed charge distributions, boundary positions and other parameters is as outlined in Figure 1 and described in the text for all three channels studied and remains the same for all results presented in this paper. Note that positive voltage corresponds to $\phi_L - \phi_R > 0$.

constant of ca. 2, the value of the appropriate dielectric constant for the protein is less certain. Various flexible polar groups in the protein suggest a polarizability that may put the dielectric constant of the protein in the range of 2−10.[40,41] Despite all of these complications, in this work we have chosen to use the dielectric constant $\varepsilon_w = 80$ for both bulk and channel-confined water and the value $\varepsilon_m = 2$ everywhere else. With such parameter choices (which are often considered as standard in the field of biomolecular simulations; see the extensive discussion in ref 23), the effect of the dielectric barrier on ion dynamics in the channel is expected to be significant.

The membrane thickness (and channel length) was taken to be 24 Å, consistent with typical lipid bilayer membrane thicknesses. Bulk 1:1 electrolyte concentrations of 0.1 M were adopted throughout. Three values of the radius of the cylinder representing the interior of the channel protein were considered, namely, $R = 4$, 7.5, and 12 Å.

All calculations presented below that require solving the Poisson equation (i.e., an evaluation of the electrostatic potential in both PNP and DLMC methods as well as an evaluation of the DSE potential for a single ion) or the Nernst−Planck equations were performed on a cubic lattice with 2-Å spacing

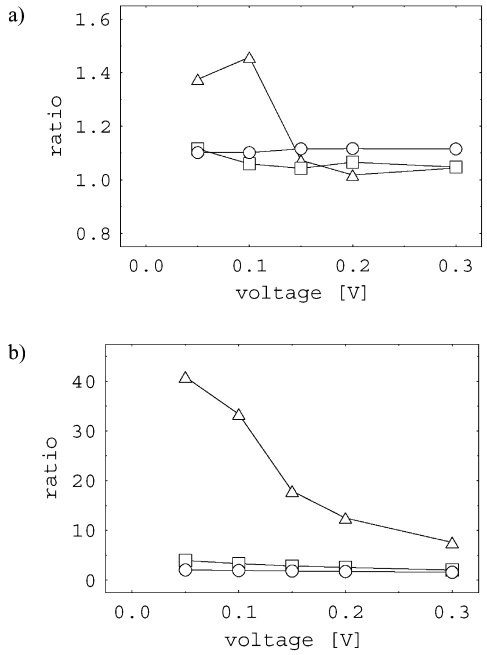


**Figure 3.** (a) Ratio of DSEPNP/DLMC currents as a function of voltage for three channel radii: 0.4 nm (triangles), 0.75 nm (squares), and 1.2 nm (circles). (b) Ratio of PNP/DLMC currents for the same channels: 0.4 nm (triangles), 0.75 nm (squares), and 1.2 nm (circles).

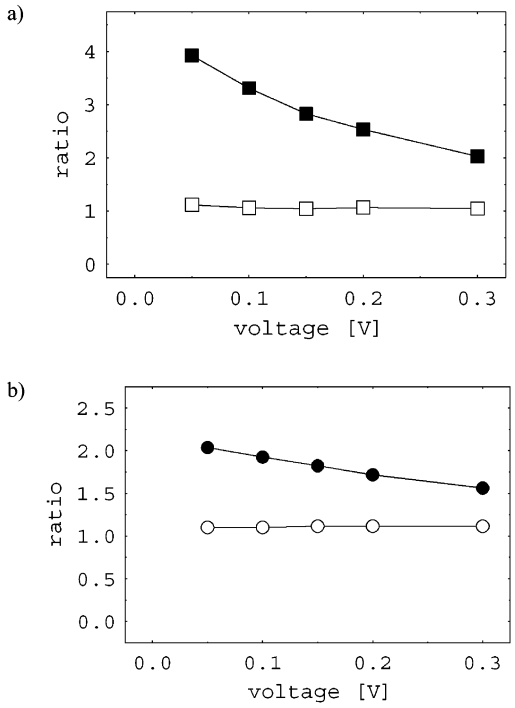


**Figure 4.** (a) Ratio of PNP/DLMC current (filled squares) and DSEPNP/DLMC current (open squares) as a function of voltage for channel radius $R = 0.75$ nm. (b) Ratio of PNP/DLMC current (filled circles) and DSEPNP/DLMC current (open circles) as a function of voltage for channel radius $R = 1.2$ nm.

between adjacent grid points. This choice also defined the size of an ion in the DLMC simulations. The charge discretization procedure on the lattice has been described in detail in ref 4.

In Figure 2, we show for each of these cylinder radii ($R = 4$, 7.5, and 12 Å in panels a, b, and c, respectively) current−voltage ($I-V$) curves obtained via DLMC simulations and compare these

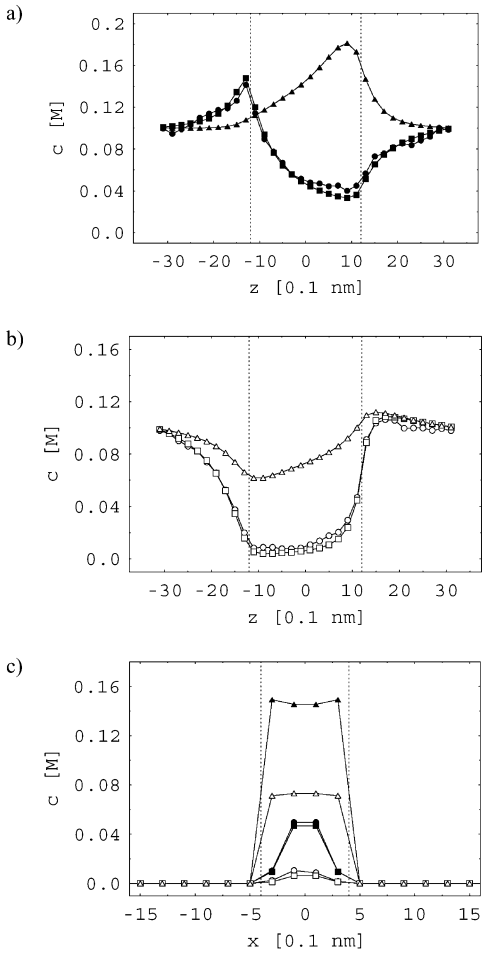


**Figure 5.** Mobile ion concentrations calculated by DLMC, DSEPNP, and PNP plotted for the $R = 0.4$ nm channel at an applied voltage of 0.3 V and a 0.1 M reservoir concentration of salt. Filled symbols are for cations; open symbols are for anions. Circles show DLMC results, squares, DSEPNP results, and triangles, PNP results: (a) positive mobile ion concentration along the (channel) $z$ axis ($x = 0$, $y = 0$); (b) negative mobile ion concentration along the $z$ axis; (c) mobile ion concentration along the (transverse) $x$ axis at the center of the channel ($z = 0$, $y = 0$).

to the predictions of DSEPNP theory. The agreement is good for all three channel radii. To quantify this claim, we show in Figure 3a the ratio of DSEPNP/DLMC currents as a function of applied voltage. Generally, the error is less than 20% (with slightly larger deviations at low voltages in the narrowest channel, $R = 4$ Å). The performance of standard PNP is dramatically worse than this, particularly for the $R = 4$ Å channel, as is shown in Figure 3b. PNP significantly overestimates the current flow relative to DLMC, with striking deviations of nearly a factor of 50 for the $R = 4$ Å channel at low voltages due primarily to its neglect of the DSE contribution to the free energy experienced by a permeating ion. For channel radii of 7.5 and 12 Å, the deviation of PNP from DLMC is more modest. To emphasize this, we replot relevant data curves from Figure 3 in Figure 4. As expected, the agreement of PNP with DLMC improves systematically with increasing channel radius: for the 12-Å channel, the error is only a factor of 2.

It is also instructive to examine the steady-state concentration distributions of the mobile ions in the channel. In Figure 5, we show for the $R = 4$ Å channel the cation (Figure 5a) and anion (Figure 5b) concentrations along the channel axis.[45] As is readily apparent, the PNP curves bear little correspondence to their

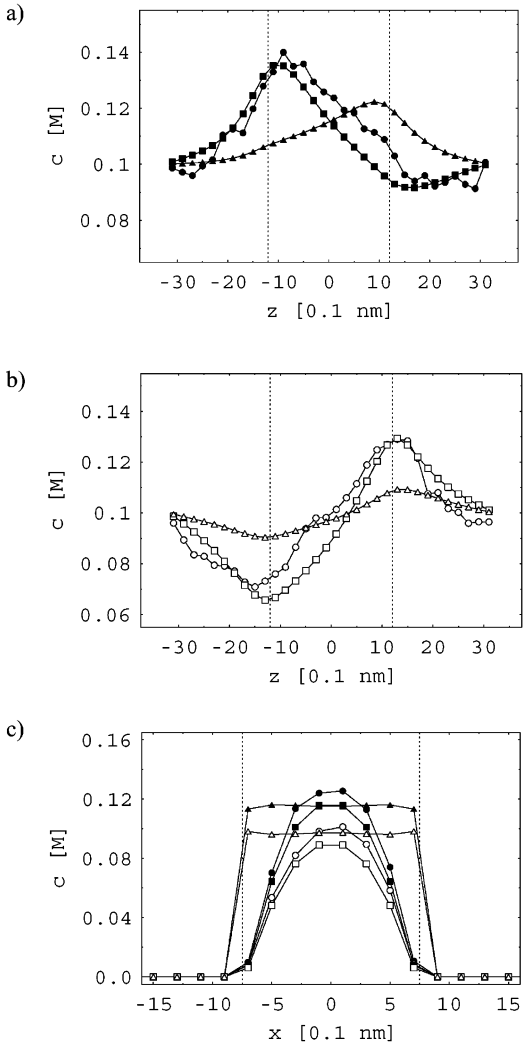


**Figure 6.** Mobile ion concentrations calculated by DLMC, DSEPNP, and PNP plotted for the $R = 0.75$ nm channel at an applied voltage of 0.3 V and a 0.1 M reservoir concentration of salt. Filled symbols are for cations; open symbols are for anions. Circles show DLMC results, squares, DSEPNP results, and triangles, PNP results: (a) positive mobile ion concentration along the (channel) $z$ axis ($x = 0$, $y = 0$); (b) negative mobile ion concentration along the $z$ axis; (c) mobile ion concentration along the (transverse) $x$ axis at the center of the channel ($z = 0$, $y = 0$).

DLMC analogues. However, the results of the DSEPNP calculation are in very good agreement with the DLMC simulation results. Figure 5c shows a lateral slice of the cation and anion densities through the center of the same channel. Again, PNP deviates substantially from DLMC, but DSEPNP results agree very well with DLMC. This cross-sectional view also shows clearly that the DSE potential is higher near the walls of the channel, thus preventing mobile ion density from accumulating there in the DLMC and DSEPNP calculations. Because the DSE is neglected in standard PNP, this effect is absent in the PNP concentration profiles, which extend almost uniformly in the lateral direction up to the channel walls. In Figure 6, we show the corresponding results for the $R = 7.5$ Å channel, and in Figure 7, results for $R = 12$ Å are presented. The same general comments apply as for the $R = 4$ Å channel case described above. As the channel gets wider, the PNP results become somewhat better, although certain artifacts of the neglect of DSE remain noticeable, for example, the nearly step-function nature of the PNP profile in the lateral direction.

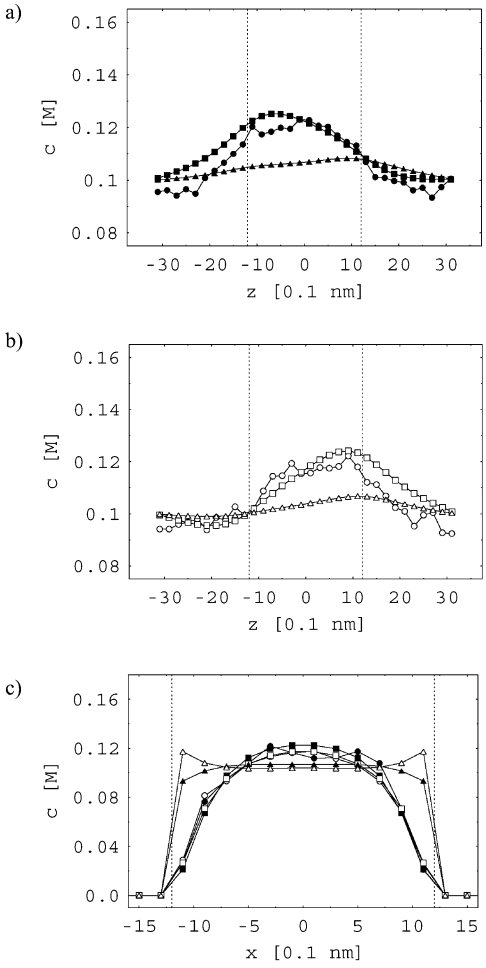


**Figure 7.** Mobile ion concentrations calculated by DLMC, DSEPNP, and PNP plotted for the $R = 1.2$ nm channel at an applied voltage of 0.3 V and a 0.1 M reservoir concentration of salt. Filled symbols are for cations; open symbols are for anions. Circles show DLMC results, squares, DSEPNP results, and triangles, PNP results: (a) positive mobile ion concentration along the (channel) $z$ axis ($x = 0$, $y = 0$); (b) negative mobile ion concentration along the $z$ axis; (c) mobile ion concentration along the (transverse) $x$ axis at the center of the channel ($z = 0$, $y = 0$).

## 6. Discussion and Conclusions

In this paper, we have studied ion permeation through biological channels within the "standard model", in which the channel is rigid, water is treated as a dielectric continuum, and the mobile ions are treated as charged spherical particles that execute Brownian motion (based on thermally driven buffeting by implicit solvent molecules). We performed dynamical Monte Carlo simulations (equivalent to Langevin dynamics at high friction) for channels ranging in radius from 4 to 12 Å. Current−voltage curves and ion concentration profiles were extracted for three channels, ranging in radius from 4 to 12 Å. These results were compared to corresponding results obtained from Poisson−Nernst−Planck (PNP) theory, in which the permeant ions are treated as a continuous charge density and the force on each ion is assumed to be static and is computed within standard mean-field theory approximations. We found, in agreement with previous calculations,[4,42] that PNP greatly overestimates the ion current through narrow channels, with the discrepancy increasing for narrower channels. The origin of this discrepancy was traced in large part to a force associated with the dielectric self-energy, which arises from the interaction of an ion with charges it induces on the dielectric boundaries. This

force is properly included in the DLMC computation but is ignored in simple PNP theory. The DSEPNP model, which takes this single ion force into account within the general framework of the PNP theory, yields $I-V$ curves and concentration profiles in nearly quantitative agreement with the corresponding DLMC simulation results for all radii studied. This suggests that other effects that are beyond the province of PNP theory (e.g., (mobile) ion−ion correlations and single-file ion queuing kinetics) affect the $I-V$ curves to only a minor degree, at least down to the minimum channel radius (4 Å) investigated here.

The above findings do not address the important issue raised in the Introduction concerning significant flaws in the "standard model", including a static representation of the channel and a continuum representation of the water solvent, especially the solvent molecules inside the channel. Because of these oversimplifications, this model predicts extremely small currents through narrow channels, in stark contradiction to experimental reality. Reference 23 suggests a practical, though approximate, way to include these effects in determining the potential of mean force (PMF), $\psi_I$ in eq 1, experienced by a permeant ion. The full PMF includes, in addition to the DSE force, a stabilizing force due to the local relaxation of the protein channel around an ion as it moves through the channel. When this full single-ion PMF is utilized as input into PNP theory (with the usual mean-field theory arguments used to simplify the effect of the force on a test ion due to all other permeant ions), the resultant PMFPNP theory predicts ion currents that are in reasonable agreement with experiment even for the very narrow gramicidin channel (radius of 2 Å). As noted in the Introduction, this is largely a consequence of the cancellation of two effects: the DSE barrier is compensated by a potential well corresponding to the "polaronic" stabilization of the ion in the channel due to local conformational relaxation of the protein. Furthermore, PMFPNP can predict[23] the saturation of ion current with increasing concentration (at fixed voltage), a property of current flow through real protein channels that does not emerge from standard PNP theory. It would be interesting to carry out calculations in which the single-particle force on each ion is obtained from a PMF calculation of the type outlined in ref 23 while the forces between all pairs of mobile ions are computed via a DLMC simulation with an accurate evaluation of the relevant electrostatic interactions. In this way, ion−ion correlation effects, single-file queuing kinetics, and so forth could be studied more carefully. Although these apparently play only a minor role in the present model system, they may be important in more chemically realistic models of narrow channels, for example, those that have selectivity filters (e.g., the KcSA channel).[6,11,22]

**Note Added in Proof.** While this paper was in review, the following papers addressing the issue of dielectric boundary forces in ion channel energetics appeared: (1) Nadler, B.; Hollerbach, U.; Eisenberg, R. S. *Phys. Rev. E* **2003**, *68*, 021905, 1−9; (2) Corry, B.; Kuyucak, S.; Chung, S. H. *Biophys. J.* **2003**, *84*, 3594−3606.

**Acknowledgment.** A.N.'s work was supported in part by the Israel Science Foundation and by the Kurt Lion Fund. Work in R.D.C.'s group was supported by NIH Grant R0l GMG1082-03 and NSF Grant CHE 0092285. M.G.K. acknowledges the financial support provided by Marquette University and the Research Corporation.

## Appendix 1: Origin of the Dielectric Self-Energy Term

The following discussion (Appendices 1 and 2) is based on idealized point charges. This idealization allows for a compact presentation of the issues that we want to focus on. We note, however, that our conceptual model and its implementation in the present and our earlier work[4] are based on finite-sized ions (i.e., spherically distributed charges[46]).

Consider a collection of $N$ point charges in an inhomogeneous dielectric medium, as sketched in Figure 1. The charges may be mobile or embedded in the medium ("fixed").

First, we calculate the electrostatic energy required to assemble this system of charges from infinite separation. For the moment, we assume that no externally applied voltage is present. The work required is[43]

$$\mathcal{E}(\vec{R}_1, ..., \vec{R}_N) = \frac{1}{8\pi}\int d\vec{r}\ \vec{E}\cdot\vec{D} \qquad \text{(A1.1)}$$

Here, $\vec{E}$ is the electric field vector. It is related to the electric potential as $\vec{E} = -\vec{\nabla}\phi$, where the scalar field $\phi(\vec{r})$ is the (unique) solution to the Poisson equation (PE) corresponding to the given collection of source charges, dielectric regions, and the boundary condition that $\phi = 0$ on all bounding surfaces (far from the charges). Specifically, the relevant PE reads

$$\vec{\nabla}\cdot(\varepsilon(\vec{r})\vec{\nabla}\phi(\vec{r})) = -4\pi\sum_{j=1}^{N} q_j\,\delta(\vec{r} - \vec{R}_j) \qquad \text{(A1.2)}$$

where on the lhs $\varepsilon(\vec{r})$ is the dielectric profile and on the rhs $q_j$ is the value of the $j$th charge and $\delta(\vec{r})$ is a three-dimensional Dirac delta function. Finally, the electric displacement vector is determined from the electric field by the proportionality relation $\vec{D}(\vec{r}) \equiv \varepsilon(\vec{r})\vec{E}(\vec{r})$.

This electrostatic energy can be equivalently expressed as follows. Integrating by parts and discarding the surface terms[47] yields

$$\mathcal{E} = \frac{1}{2}\sum_{j=1}^{N} q_j\,\phi(\vec{R}_j) \qquad \text{(A1.3)}$$

Next, we examine $\phi$ in more detail. Because the PE is linear, the overall potential is composed of contributions from each of the source terms

$$\phi(\vec{r}) = \sum_{j=1}^{N} q_j\, g(\vec{r},\vec{R}_j) \qquad \text{(A1.4)}$$

where $g(\vec{r},\vec{R}_j)$ is the potential generated at point $\vec{r}$ by a unit source charge at point $\vec{R}_j$, i.e., the solution of

$$\vec{\nabla}\cdot(\varepsilon(\vec{r})\vec{\nabla}g) = -4\pi\delta(\vec{r} - \vec{R}_j) \qquad \text{(A1.5)}$$

subject to the boundary condition that $g \to 0$ far from $\vec{R}_j$. Note that in a homogeneous medium characterized by dielectric constant $\varepsilon$ and far away from any boundary surfaces

$$g(\vec{r},\vec{R}_j) = \frac{1}{\varepsilon|\vec{r} - \vec{R}_j|} = g(\vec{r} - \vec{R}_j) \qquad \text{(A1.6)}$$

That is, the standard Coulomb potential is recovered. If the medium is *in*homogeneous, however, then the function $g(\vec{r},\vec{R}_j)$ depends on where the source charge $\vec{r}$ is located with respect to the dielectric inhomogeneities in the medium and on the orientation of the test point $\vec{r}$ as well as its distance from the source charge. In general, $g$ must be obtained by solving eq A1.5 numerically. However, even in the inhomogeneous medium case, $g$ retains the symmetry property that $g(\vec{r},\vec{R}_j) =$

$g(\vec{R}_j,\vec{r})$ (because the operator $\vec{\nabla}\varepsilon\vec{\nabla}$ is symmetric). Substituting eq A1.4 into A1.3, we obtain

$$\mathcal{E}(\vec{R}_1, ...,\vec{R}_N) = \frac{1}{2}\sum_{j=1}^{N}\sum_{k=1}^{N} q_j q_k g(\vec{R}_j,\vec{R}_k) \qquad \text{(A1.7)}$$

The double sum on the rhs can be separated into diagonal and off-diagonal terms

$$\mathcal{E} = \sum_{j<k} q_j q_k g(\vec{R}_j,\vec{R}_k) + \frac{1}{2}\sum_{j=1}^{N} q_j^2 g(\vec{R}_j,\vec{R}_j) \qquad \text{(A1.8)}$$

where the first sum includes contributions from all pairs of charges and we have used the symmetry property of $g$ noted above. The first term is essentially the potential energy obtained by summing Coulomb-like pair potentials (suitably modified to take account of the dielectrically inhomogeneous medium), and the second term includes the self-energy associated with each ion.

The force on a given mobile ion, say ion $n$, is determined as the gradient of the "single-ion energy". To determine this, we need to retain only the terms in eq A1.8 that depend on $\vec{R}_n$:

$$\mathcal{E}'(\vec{R}_n) = q_n \sum_{j\neq n} q_j g(\vec{R}_n,\vec{R}_j) + \frac{1}{2} q_n^2 g(\vec{R}_n,\vec{R}_n) \qquad \text{(A1.9)}$$

The first term in this equation is the potential energy experienced by test charge $n$ due to all of the other free charges in the system. The second term is the dielectric self-energy (DSE) of test charge $n$. In a dielectrically inhomogeneous medium, the DSE depends on the location of the test charge in the medium and hence contributes to the force experienced by charge $n$ as it moves through the system.

## Appendix 2: Connection between Dielectric Self-Energy and Dielectric Boundary Force

The electrostatic energy needed to assemble a collection of free charges in a dielectric medium can be written in general as[48,49]

$$\mathcal{E} = \frac{1}{2}\int \rho\phi \, d\vec{r} = \int \rho\phi \, d\vec{r} + \frac{1}{8\pi}\int \phi\vec{\nabla}\cdot(\varepsilon\vec{\nabla}\phi) \, d\vec{r} \qquad \text{(A2.1)}$$

Suppose that there is a point charge $q$ at position $\vec{R}_0$. We seek to calculate the change in $\mathcal{E}$ if $q$ is moved by a small distance to $\vec{R}_0 + \delta\vec{R}$. We can do this as follows. First, calculate the electric potential field $\phi(\vec{R})$ generated by point charge $q$ at $\vec{R}_0$ subject to the boundary condition that $\phi \to 0$ far from the point source. In other words, solve the Poisson equation

$$\vec{\nabla}\cdot(\varepsilon(\vec{r})\vec{\nabla}\phi(\vec{r})) = -4\pi\rho(\vec{r}) \qquad \text{(A2.2)}$$

with $\rho(\vec{r}) = \delta(\vec{r} - \vec{R}_0)$ and the boundary condition just noted. Now move the charge by $\delta\vec{R}$. For a sufficiently small change in position, the electrostatic energy changes by[50]

$$\delta\mathcal{E} = \int(\delta\rho\phi + \rho\delta\phi)d\vec{r} + \frac{1}{8\pi}\int(\delta\phi\nabla\varepsilon\nabla\phi + \phi\nabla\varepsilon\nabla\delta\phi) \, d\vec{r} \qquad \text{(A2.3a)}$$

$$= \int \delta\rho\phi \, d\vec{r} + \int \delta\phi\left(\rho + \frac{1}{4\pi}\nabla\varepsilon\nabla\phi\right) d\vec{r} \qquad \text{(A2.3b)}$$

where to obtain eq A2.3b we have used the symmetry of the operator $\nabla\varepsilon\nabla$. Note that the quantity in parentheses in the second integral appearing in eq A2.3b vanishes identically because $\phi$ satisfies the Poisson equation (eq A2.2). Thus,

$$\delta\mathcal{E} = \int \delta\rho\phi \, d\vec{r} = q\left(\phi(\vec{R}_0 + \delta\vec{R}) - \phi(\vec{R}_0)\right) \qquad \text{(A2.4)}$$

The first equality holds for *any* change in an arbitrary charge distribution, and the second specializes to the case under consideration here, where $\delta\rho = q\left(\delta(\vec{r} - [\vec{R}_0 + \delta\vec{R}]) - \delta(\vec{r} - \vec{R}_0)\right)$. Equation A2.4 is clearly equivalent to the statement

$$\vec{\nabla}\mathcal{E}(\vec{R})_{|\vec{R}=\vec{R}_0} = q\vec{\nabla}\phi(\vec{r})_{|\vec{r}=\vec{R}_0} \qquad \text{(A2.5)}$$

which establishes a nontrivial relation between the gradient of the dielectric self-energy of a point charge at point $\vec{R}_0$ and the electric potential $\phi$ generated by a point charge at $\vec{R}_0$.[51]

Note that eq A2.5 gives the force on a test charge at $\vec{R}_0$ due to an arbitrary collection of free charges in a dielectrically inhomogeneous medium. Here we are primarily interested in the situation where there are no free charges in the system besides the test charge at $\vec{R}_0$. In this case, $\mathcal{E}(\vec{R}) = (1/2)q^2 g(\vec{R},\vec{R})$, and $\phi(\vec{r})$ on the rhs of eq A2.5 is the solution of the PE for a source charge at $\vec{R}_0$ (and $\phi(\vec{r}) \to \infty$ far away from this source charge). This establishes the equivalence between the DSE perspective adopted in the present work (the lhs of eq A2.5 specialized to the case of one free charge at $\vec{R}_0$) and the dielectric boundary force perspective of Schuss et al. (rhs of eq A2.5 under similar conditions[35]).

## References and Notes


(1) Chung, S. H.; Hoyles, M.; Allen, T.; Kuyucak, S. *Biophys. J.* **1998**, *75*, 793−809.
(2) Chung, S. H.; Allen, T. W.; Hoyles, M.; Kuyucak, S. *Biophys. J.* **1999**, *77*, 2517−2533.
(3) Allen, T. W.; Hoyles, M.; Kuyucak, S.; Chung, S. H. *Chem. Phys. Lett.* **1999**, *313*, 358−365.
(4) Graf, P.; Nitzan, A.; Kurnikova, M. G.; Coalson, R. D. *J. Phys. Chem. B* **2000**, *104*, 12324−12338.
(5) Im, W.; Seefeld, S.; Roux, B. *Biophys. J.* **2000**, *79*, 788−801.
(6) Mashl, R. J.; Tang, Y. Z.; Schnitzer, J.; Jakobsson, E. *Biophys. J.* **2001**, *81*, 2473−2483.
(7) Kuyucak, S.; Andersen, O. S.; Chung, S. H. *Rep. Prog. Phys.* **2001**, *64*, 1427−1472.
(8) Allen, T. W.; Chung, S. H. *BBA-Biomembranes* **2001**, *1515*, 83−91.
(9) Im, W.; Roux, B. *J. Chem. Phys.* **2001**, *115*, 4850−4861.
(10) Roux, B. *Curr. Opin. Struct. Biol.* **2002**, *12*, 182−189.
(11) Burykin, A.; Schutz, C. N.; Villá, J.; Warshel, A. *Proteins: Struct. Funct. Genet.* **2002**, *43*, 265−280.
(12) Corry, B.; Allen, T. W.; Kuyucak, S.; Chung, S. H. *Biophys. J.* **2001**, *80*, 195−214.
(13) Andersen, O. S.; KoeppeII, R. E. *Physiol. Rev.* **1992**, *72*, S89−S158.
(14) Busath, D. D.; Thulin, C. D.; Hendershot, R. W.; Phillips, L. R.; Maughan, P.; Cole, C. D.; Bingham, N. C.; Morrison, S.; Baird, L. C.; Hendershot, R. J.; Cotten, M.; Cross, T. A. *Biophys. J.* **1998**, *75*, 2830−2844.
(15) Barcilon, V.; Chen, D. P.; Eisenberg, R. S. *SIAM J. Appl. Math.* **1992**, *53*, 1405−1425.
(16) Chen, D. P.; Eisenberg, R. S. *Biophys. J.* **1993**, *65*, 727−746.
(17) Chen, D. P.; Eisenberg, R. S. *Biophys. J.* **1993**, *64*, 1405−1421.
(18) Kurnikova, M. G.; Coalson, R. D.; Graf, P.; Nitzan, A. *Biophys. J.* **1999**, *76*, 642−656.
(19) Cardenas, A. E.; Coalson, R. D.; Kurnikova, M. G. *Biophys. J.* **2000**, *79*, 80−93.
(20) Hollerbach, U.; Chen, D. P.; Busath, D. D.; Eisenberg, B. *Langmuir* **2000**, *16*, 5509−5514.
(21) Arsen'ev, A. S.; Lomize, A. L.; Barsukov, I. L.; Bystrov, V. F. *Biol. Membr.* **1986**, *3*, 1077−1104.
(22) Doyle, D. A.; Cabral, J. M.; Pfuetzner, R. A.; Kuo, A. L.; Gulbis, J. M.; Cohen, S. L.; Chait, B. T.; MacKinnon, R. *Science* **1998**, *280*, 69−77.
(23) Mamonov, A.; Coalson, R. D.; Nitzan, A.; Kurnikova, M. G. *Biophys. J.* **2003**, *84*, 3646−3661.
(24) Dieckmann, G. R.; Lear, J. D.; Zhong, Q. F.; Klein, M. L.; DeGrado, W. F.; Sharp, K. A. *Biophys. J.* **1999**, *76*, 618−630.

(25) Parsegian. A. *Nature* **1969**, *221*, 844−845.
(26) Levitt, D. G. *Biophys. J.* **1978**, *22*, 209−219.
(27) Jordan, P. C. *Biophys. J.* **1983**, *41*, 189−195.
(28) Cooper, K.; Jakobsson, E.; Wolynes, P. *Prog. Biophys. Mol. Biol.* **1985**, *46*, 51−96.
(29) Jakobsson, E.; Chiu, S. W. *Biophys. J.* **1987**, *52*, 33−45.
(30) Jakobsson, E.; Chiu, S. W. *Biophys. J.* **1988**, *54*, 751−756.
(31) Partenskii, M. B.; Jordan, P. C. *Q. Rev. Biophys.* **1992**, *91*, 477−480.
(32) Partenskii, M. B.; Dorman, V.; Jordan, P. C. *Biophys. J.* **1994**, *67*, 1429−1438.
(33) Cheng, W.; Wang, C. X.; Chen, W. Z.; Xu, Y. W.; Shi, Y. Y. *Eur. Biophys. J. Biophys. Lett.* **1998**, *27*, 105−112.
(34) Kittel, C. *Introduction to Solid-State Physics*, 7th ed.; Wiley: New York, 1996.
(35) Schuss, Z.; Nadler, B.; Eisenberg, R. S. *Phys. Rev. E* **2001**, *64*, 036116, 1−14.
(36) McQuarrie, D. A. *Statistical Mechanics*; HarperCollins: New York, 1976.
(37) Eisenberg, R. S. *J. Membr. Biol.* **1996**, *150*, 1−25.
(38) Sharp. K. A.; Honig B. H. *Annu. Rev. Biophys. Biophys. Chem.* **1990**, *19*, 301−332.
(39) Binder K. *Phase Transitions and Critical Phenomena*; Academic Press: New York, 1976; Chapter 1, pp 1−105.
(40) Gilson, M. K.; Honig B. H. *Biopolymers* **1986**, *25*, 2097−2119.
(41) Schutz, C. N.; Warshel, A. *Proteins: Struct. Funct. Genet.* **2001**, *44*, 400−417.
(42) Corry, B.; Kuyucak, S.; Chung, S. H. *Chem. Phys. Lett.* **2000**, *320*, 35−41.
(43) Jackson, J. D. *Classical Electrodynamics*, 2nd ed.; Wiley: New York, 1975.

(44) In reality, $D$ is expected to be different in the bulk and inside the channel, but this distinction is not important in the present context.

(45) To obtain each point on this curve, an average was taken over the central point (along the $z$ axis) and its four nearest-neighbor grid points in the $x-y$ plane.

(46) Such a finite-sized ion model has the following advantages: (1) It renders all self-energies, and forces derived from these, finite. Therefore, a renormalization of infinite self-energies is not necessary. (2) It inherently encompasses the "Born solvation energy" for a nonuniform dielectric.

(47) These surface terms can be discarded because of the boundary condition that $\phi = 0$ on all bounding surfaces. Note also that the Poisson equation (eq A1.2) has been invoked in order to obtain eq A1.3.

(48) This derivation parallels the treatment of M. K. Gilson, M. E. Davis, B. A. Luty, and J. A. McCammon (*J. Phys. Chem.* **1993**, *97*, 3591), who were interested in the force on a macroion in an electrolytic solution.

(49) Note: $(1/2)\int \rho\phi \, d\vec{r} = (1/8\pi)\int \vec{E}\cdot\vec{D} \, d\vec{r} = (-1/8\pi)\int \phi\vec{\nabla}\cdot(\varepsilon\vec{\nabla}\phi) \, d\vec{r}$, where $\phi$ solves the Poisson equation for source charge density $\rho$ and boundary condition $\phi = 0$ on all bounding surfaces and $\vec{E}$ and $\vec{D}$ are related to $\phi$ in the usual manner.

(50) This assumes no changes in the dielectric function as the charged body in question moves. This assumption is valid for the case of a point ion moving through a medium that is locally uniform (e.g., the solvent).

(51) Note: The "homogeneous Coulomb potential" term that is subtracted from this $\phi$ in Schuss' formulation does not contribute to the dielectric force. (Its derivative in any direction is zero at the source singularity $\vec{r} = \vec{R}_0$.)